ce/papers Proceedings in civil engineering

Ernst & Sohn A Wiley Brand

ORIGINAL ARTICLE

ibausil F. A. Finger-Institut für Baustoffkunde Bauhaus-Universität Weimar

Spatially resolved *in situ* analyses of the adsorption behavior of different admixtures on binders

Denis Kosenko[1] | Alexander Wetzel[1] | Bernhard Middendorf[1]

Correspondence

Denis Kosenko
University of Kassel
Inst. for Structural Engineering
Dept. of Structural Materials and Construction Chemistry
Mönchebergstraße 7
34125 Kassel
Email: denis.kosenko@uni-kassel.de

[1] University of Kassel, Kassel, Germany

Abstract

Admixtures play a key role in improving the performance of the cement paste matrix. A more efficient matrix can allow a reduction the binder content while maintaining the same properties. There is currently a lack of knowledge about the spatial distribution of admixtures *in situ* on binder surfaces which would facilitate the use of admixtures in general in inorganic binder systems. Imaging techniques such as confocal laser scanning microscopy (CLSM) and fluorescence microscopy can be used to study the spatiotemporal adsorption of superplasticizers and plasticizers on binder particles. However, in order to make the admixtures visible using these methods, they must first be coupled to a fluorescent molecule (staining). Different types of superplasticizers and plasticizers, including polycarboxylate ethers (PCE) and lignosulfonate (LS) were stained and tested. It was shown that not only adsorption but also desorption can be observed and that desorption cannot play a relevant role in a binder system. The absence of desorption could be used to observe a real system in permanent preparations, so that the adsorption on individual cement grains could be followed in a time-dependent manner. The newly developed method provides unprecedented insight into the adsorption of additives.

Keywords

superplasticizers, confocal laser scanning microscopy, lignosulfonate, polycarboxylate ether, fluorescence microscopy, adsorption

1 Introduction

About 9 % of total CO_2 emissions worldwide are caused by concrete production, of which 75 % are due to cement production [1]. Reducing the use of cement thus reduces emissions. This can be achieved by the addition of supplementary cementitious materials (SCM) to cement, or by using alternatives where the cement is fully substituted entirely by latent hydraulic or pozzolanic binders or by using alkali activated materials (AAM) [2] or geopolymers [3] which can reduce the climate footprint [4–6]. Additional, by increasing the performance of the cement paste matrix, the cement content can also be reduced with consistent properties.

However, there is a lack of numerous admixtures for applications at low w/b ratios. Superplasticizers, particularly polycarboxylate ethers, are an essential type of admixture that is well known to be high effective in cementitious systems [7]. Lignosulfonate (LS) can also improve the rheological properties and reduce the water demand of a cementitious or alternative system, especially in alkaline milieu [8, 9]. The admixtures mentioned are surface-active, which means that their adsorption on particles plays a key role in their mode of action. In the past, the adsorption of superplasticizers on binder particles has only been indirectly determined in most publications, for example by measuring the total organic carbon (TOC) or the zeta potential [10–15].

A new analytical approach using fluorescence microscopy enables the visualization of the adsorption of superplasticizers on inorganic surfaces in a spatially resolved manner. For cementitious systems, the relationship between the zeta potential, adsorption, dissolved Na^+, K^+ and Ca^{2+} ions and slump has already been demonstrated [16] *in situ* using simple setups and stained PCE superplasticizer. Due to the chosen setup, these investigations were limited in some respects. Further development of this setup was necessary so that even the finest particles, which had to be washed out in previous publications, can be analysed.

Adsorption studies in a flow cell will give an impression of the adsorption and desorption of the admixtures mentioned. These results will be used to make permanent preparations for the study of a simple, real system using a CLSM. However, for the verification of the new method, simplified tests will be performed to reflect the known ad-

https://doi.org/10.1002/cepa.2798

sorption behaviour on cement. In addition to the measurements, a new method is being developed to extend the staining reaction to another class of admixtures, lignosulfonates. However, the newly developed methods should allow the analysis to be extended to finer binder types. This makes it possible to analyse metakaolin and silica fume, whose effect on the liquefaction of admixtures has been widely studied but not yet fully deciphered.

2 Materials and methods

2.1 Raw materials

2.1.1 Powders

The specific surface areas S_m of the powders were determined after Blaine according to German standard DIN 66126-2, and the particle sizes were determined by laser granulometry. The densities were measured by helium pycnometry. Quartzpowder was purchased from Quarzwerke GmbH, Germany, and had an S_m value of 3800 cm^2/g, a density of ρ = 2.7 g/cm^3, and a median particle size d_{50} of 16.9 µm. The white cement used was obtained from Dyckerhoff, Germany, and had a specific surface[1)] of 3628 cm^2/g, a density[1)] of ρ = 2.9 g/cm^3, and a d_{50} value of 14.9 µm. The fly ash was purchased from BauMineral, Germany, and had a specific surface area of 2770 cm^2/g, a density of ρ = 2.3 g/cm^3, and a d_{50} value of 11.0 µm. The chemical compositions can be found in table 1.

Table 1 Chemical compositions of the powders (wt. %)

type	CaO	SiO_2	Al_2O_3	Fe_2O_3	SO_3
cement[1)]	65	22	5	<1	3
fly ash	6	51	35	5	1
quartzpowder	<1	99	<1	<1	-

1) Data from Dykerhoff, Mainz-Amöneburg, Germany

2.1.2 Admixtures

A Lignosulfonate and a PCE of type 52IPEG4.5 was obtained from Prof. Plank's group at the Department of Chemistry at the TU Munich. The PCE has an average chain length of 52 (-CH2-CH2-O-) units and a ratio of 4.5 -COOH/side chain.

2.2 Staining of PCE

In order to observe the PCE in a fluorescence microscope or a confocal laser scanning microscope CLSM, a staining reaction was performed. This reaction involves attaching a fluorochrome, aminofluorescein (AmF), to a PCE molecule (1) through a covalent bond. The reaction, illustrated in Figure 1, involves the formation of a reactive intermediate (3) from the PCE using 1-Ethyl-3-(3-dimethylaminopropyl)carbodiimide (EDC) (2). The intermediate can then couple with a primary aromatic amine to produce a fluorescent PCE-marker molecule (4). During the reaction, a byproduct urea species (5) is formed. This byproduct can be separated from the desired product through dialysis due to its large difference in molar mass compared to the PCE.

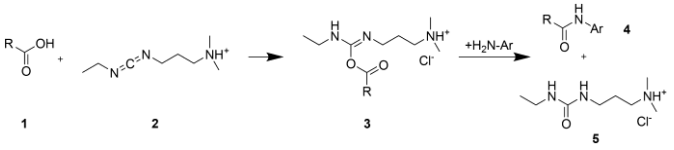

Figure 1 Staining of a PCE molecule

After taring a 100 ml round bottom flask on a scale, 4 g calculated from the respective solid content of the PCE are given into the flask and filled up to 48 g. In a vial, 5.2mg (1.5 · 10-5 mol) 5-Aminofluorescein (AmF) was dissolved in 1 ml DMSO (only for transfer) and given to the flask. 28.8 mg (1.5 · 10-4 mol) 1-Ethyl-3-(3-dimethylaminopropyl)carbodiimide (EDC) was dissolved in 1 ml MES buffer and given to the solution. The reaction mixture was stirred for 5 days at room temperature. After stirring, the mixture was given into a dialysis tube with a molecular weight cut-off (MWCO) of 3,5 kDa and fixed with locking clamps. The filled dialysis-tube was fixed in a 5 l bucket and filled up to 4.5 l and stirred for five days with everyday water exchange. After four days, the dialysis water was clear. The product has been vacuum dried to mass consistency.

2.3 Staining of Lignosulfonate

Lignosulfonate has several primary alcohols that can be oxidized to carboxylic acids on contact with oxygen. Figure 2 shows an example of a section of the lignin molecule (6) [17], which contains a carboxylic acid group after oxidation with potassium permanganate (7). The arrangement of the functional groups varies in reality, but this is of no significance since the reaction only requires the availability of primary alcohols.

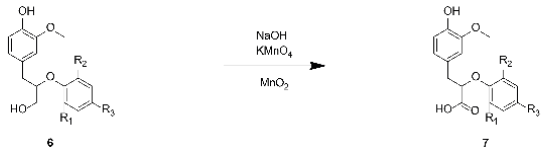

Figure 2 Oxidation of a hydroxy group on lignosulfonate

The staining reaction described in section 2.2 takes place on molecules that have a carboxylic acid group and can analogously be used for staining of oxidized lignosulfonate (7). The success of the reaction can be verified using fluorescence spectroscopy.

2.4 Measurement Setups

The imaging was performed on two different setups. One was performed in the wet, where the activator solution/water with the superplasticizer was brought into contact with fixed particles. The other setup was made by separating the particles covered with superplasticizer from a pasty mixture with a defined w/b ratio.

2.4.1 Observation in situ

With the aid of a flow cell, the adsorption of the superplasticizer can be observed *in situ*. By fixing the particles in a solid embedding medium, even the smallest particles can be observed, as they are separated from each other, which was an unsolved challenge in previous publications [18, 19]. To separate the particles, 0.15 g of each species was

placed in vials and made up to 10 g with isopropanol. Ultrasound was then applied for 120 s and 5 drops of the suspension were placed on a coarse-pored filter and allowed to dry to obtain a spot of particles on the filter surface. *M-GLAS* from Merck was used as the coating material for particle fixation. For this purpose, 0.2 ml of the solution was spin-coated on a glass slide at 5000 rpm for 3 s. Immediately after the coating process, binder particles were deposited from a dry filter on the uncured coating surface in an air stream. As shown in Figure 3, the coated object carrier was sealed with a 25 µm thick, double-sided adhesive kapton film and covered with a polystyrene object carrier with inlets equipped with nanoports [20].

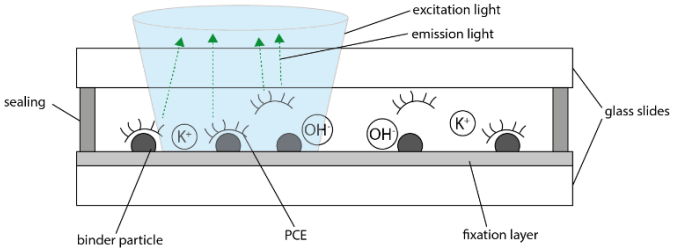

Figure 3 Measurement setup of particles in contact to activator solution in a flow cell

2.4.2 Permanent preparations

Several problems arise when considering fixed particles in the wet. It is difficult to infer a w/b ratio, as well as the dosage of the superplasticizer compared to a real system is only possible on the basis of the superplasticizer concentration in the pore solution. In microscopy, errors occur due to overexposure by the surrounding solution, since the solution also fluoresces. With permanent preparations, the admixture distribution on particles of a real paste at a certain point in time can be displayed. Due to the very slow desorption, particles can be washed from a paste, separated and fixed in an embedding medium in the same way as described in section 2.4.1. By covering the sample with a cover glass, an insensitive, dry preparation is obtained like shown in which permits measurements on a CLSM with a distance of 350 nm between the focal planes like indicated in Figure 4. To make a permanent preparation with cement, 500 mg of cement is added to an Eppendorf tube containing 5 mg of dry PCE and 250 mg of deionized water. The vessel is mixed on a vortex mixer for 20 minutes, then the paste is transferred to a centrifuge tube and centrifuged at 3000 rpm for 5 minutes. The supernatant is discarded. To wash out the excess of dissolved PCE, the sediment is suspended in 10 ml of isopropanol and centrifuged again for 5 minutes. The washing procedure is repeated twice.

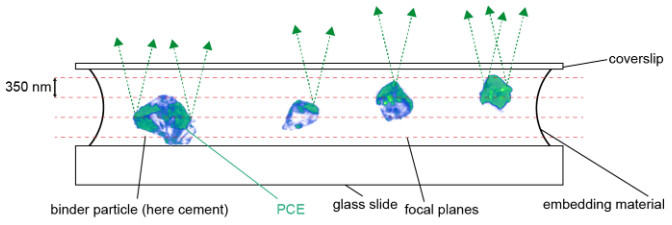

Figure 4 Measurement setup of the flow cell in CLSM

3 Results

3.1 Staining reaction

The success of staining with PCE is already well known, the products used in this work were tested by analysing the emission peak using fluorescence spectroscopy [16, 21, 22, 19]. The success of the reaction and the purity of the product when staining lignosulfonate can be checked by comparing the fluorescence spectra of an untreated reference sample, an unoxidized blank sample to which staining has been applied, and an oxidized and stained sample which were equally treated. The spectra can be seen in Figure 5.

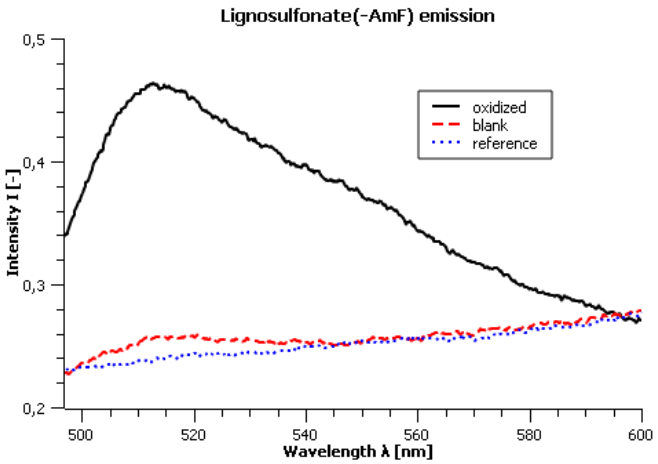

Figure 5 Fluorescence emission spectra (corrected) of LS samples at a concentration of 0.25 mg/g recorded at an excitation wavelength of 490 nm

The concentration was set to 0.25 mg/g for the measurements, since the emission decreases with increasing concentration due to the inner filter effect caused by the strong colour of lignosulfonate. However, at the concentrations used, the fluorescence intensity is sufficient for microscopic measurements. The emission spectra in Figure 5 show that the intensities of the blank and reference sample are almost identical; no peak attributable to AmF can be detected in either measurement. In contrast, the oxidized sample shows a clear peak at 517 nm, corresponding to a shift of about 4 nm compared to unreacted AmF. The result thus shows that chemically uncoupled aminofluorescein is indeed removed by dialysis, which means that AmF coupled to LS is not only physically sorbed, and therefore the coupling reaction must also occur with oxidized LS as described for PCE.

3.2 Flow cell

The flow cell can be used to bring the fixed particles into contact with changing, defined solutions. The solution with the respective stained admixture itself has a fluorescence that can complicate the analysis of the fluorescence on the particles, as can be seen in Figure 6a. After a short adsorption time of a few minutes, the superplasticizer can be almost completely washed off the particle so that fluorescence is no longer detectable. However, if the particles are kept in contact with the solution for a longer period of time (>10 min), the fluorescence signal remains almost un-

changed. To avoid incorporation of the fluorescent molecules into the reaction products possibly formed on the binder particle surfaces, inert quartzpowder particles were chosen for a desorption test. Figure 6a shows the fluorescence image of the particles in a solution of stained LS after an exposure time of 30 min. The image appears overexposed due to the background caused by the fluorescence of the solution. Due to the fixation in the flow cell, the sample can be rinsed with water. After a further waiting period of 30 minutes to allow sufficient time for desorption, the image in 6b was acquired. The background signal is now vanishingly small, and the fluorescence on the particle can be seen very clearly.

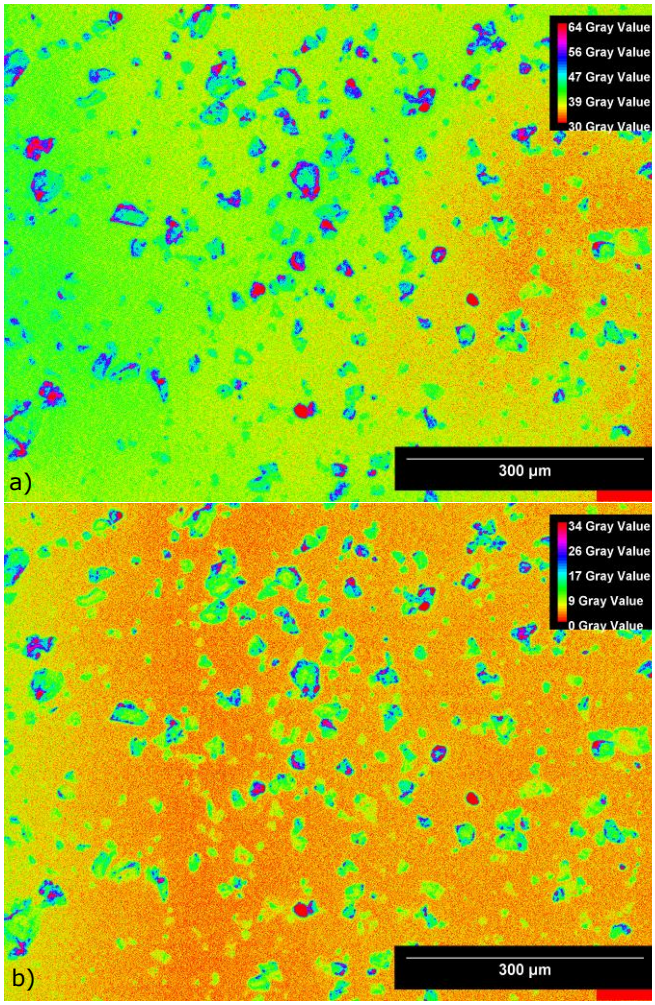

Figure 6 Fluorescence signal in false colour representation on quartz particles a) after 30 min exposure to solution b) after exposure to water for 30 min

This observation means that the apparently very slow desorption can be exploited for further attempts. For further confirmation, the mean value of the signal on the particle surface was taken as a measure to quantify the adsorption. A 0.1% stained LS solution was added to the fixed fly ash particles and allowed to adsorb for 30 min. A non-fluorescent LS solution was then extensively rinsed and measured (measurement 1). Before measurement 2, the solution was rinsed with water and measured immediately. After waiting 30 minutes in water, the solution was measured again (measurement 3). The averaged signal of the measurements can be seen in figure 7.

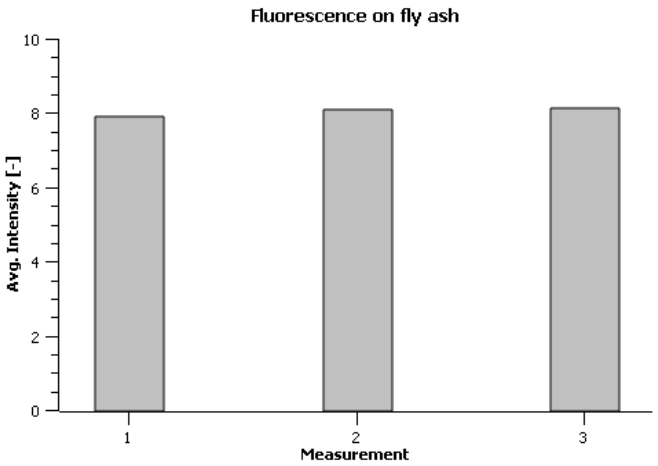

Figure 7 Averaged intensities of different rinse passes on fixed fly ash particles

It can be seen that the adsorbed molecules do not desorb measurably within the time period considered. However, this does not mean that desorption does not occur. For example, a slight decrease in fluorescence intensity was observed for quartz particles. From these results, it was concluded that unsorbed superplasticizer can be washed out of a suspension so that the particles can be observed in the dry state.

3.3 Permanent preparations

3.3.1 Fluorescence microscopy

Since the adsorption of superplasticizers on binder particles in AAM is relatively low, and the chemical nature of the particles of a given binder is relatively homogeneous, a cement was chosen for high-resolution analysis to more accurately identify the differences in distribution of the admixture on binder particles in permanent preparations. Since in cementitious systems the superplasticizer adsorption in the first few minutes is largely dependent on the very rapid formation of primary ettringite ($3CaO \cdot Al_2O_3 \cdot 3CaSO_4 \cdot 32H_2O$) by the C3A phase ($3CaO \cdot Al_2O_3$), a white cement was chosen for simplicity [23]. The remaining phases, alite ($3CaO \cdot SiO_2$) and belite ($2CaO \cdot SiO_2$), play a minor role at this stage and are only slightly occupied by the PCE. Samples were prepared after 5 and 20 minutes hydration times. The fluorescence signal shows the distribution of the PCE in the fluorescence microscope in Figure 8.

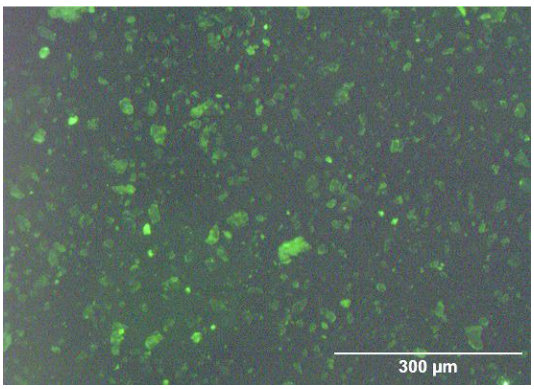

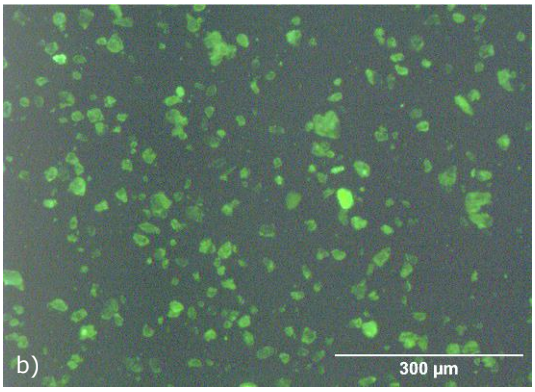

Figure 8 Fluorescence image of PCE on cement particles (brightened) after a) 5 minutes and b) after 20 minutes hydration time (w/b = 0.5, 1 wt.% PCE)

The grains show a highly inhomogeneous distribution of PCE in both images. Due to the fixed focal plane and insufficient resolution, the situation of an individual grain can only be guessed at. However, it can be seen in these overview images that both the mean intensity and the particle radius increase as hydration progresses (Fig. 8b).

3.3.2 CLSM

A confocal laser scanning microscope can be used to obtain 3-dimensional images of the particles. As with fluorescence microscopy, only the superplasticizer is visible, so the distribution of the superplasticizer is observed. The top view in Figure 9a shows some short hydrated cement grains. In particular, the larger grain on the lower left clearly shows that strong adsorption occurred on the left side of the grain, while the right side is only indicated. However, the particle is clearly visible even not the whole surface is occupied by the PCE, as shown by the two smaller grains in the upper left of the image. The largest grain in the image section shown has several areas of high adsorption. Looking at the 3D image in parallel (Fig. 9b), it is noticeable that the areas shown in green have some roughness, which may indicate freshly formed ettringite, but the resolution is not sufficient to see the known nanocrystalline needle structure.

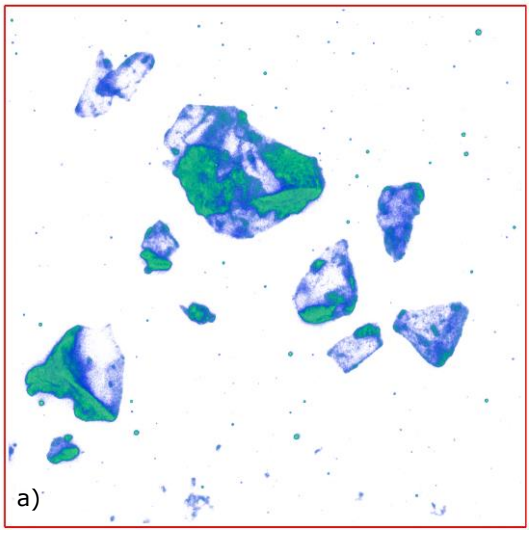

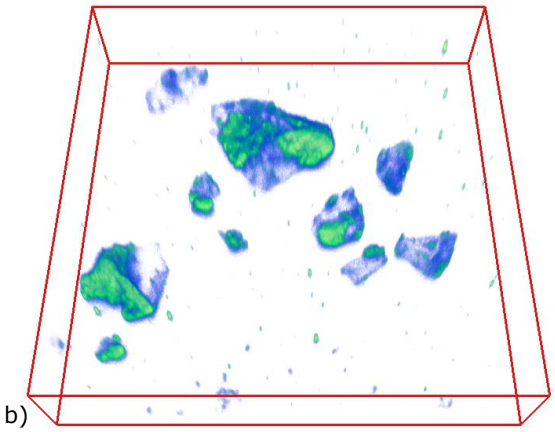

Figure 9 a) top b) side view on cement particles in false colour representation in a 74.97x74.97x16.8 µm bounding box (w/b = 0.5, 1 wt.% PCE)

Since the signal is provided solely by the PCE, it is not possible to analyse the distribution of occupied and unoccupied particle areas. Only particles can be compared with each other by integrating the relative gray values of the voxels of a respective grain. To illustrate this, 5 particles have been selected in Figure 10a where very strong to weak adsorption values can be seen with the naked eye based on the summed projection. The integrals calculated for the total particle volume in Figure 10b correlate with the observation.

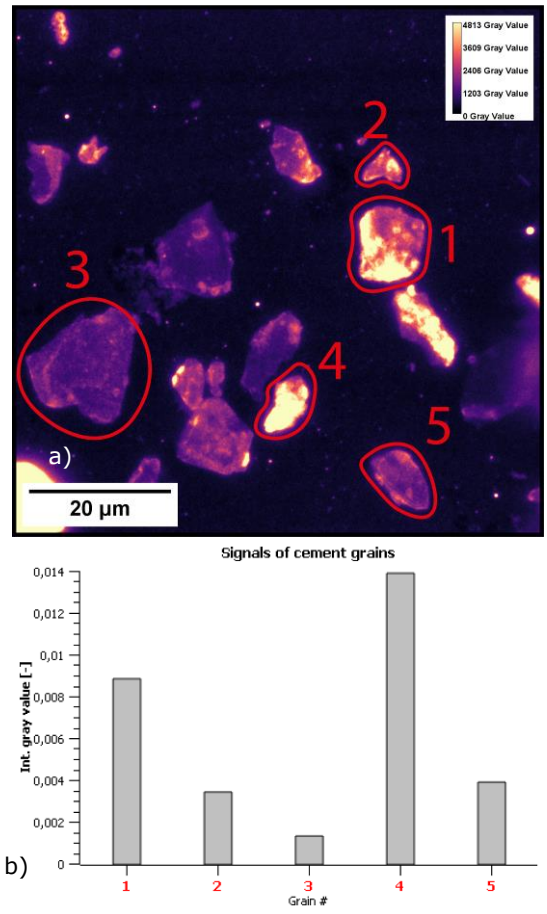

Figure 10 a) Projection of cement grains in false colour representation (w/b = 0.5, 1 wt.% PCE) and b) the resulting integrated gray values of the marked grains

With longer hydration (20 minutes), larger PCE accumulations are seen on the surface, surrounding the particles to a greater extent. At this point the crystallization of the ettringite has progressed, as shown by the green, rough structures in Figure 11. Compared to the green areas in Figure 9, the structures continue to grow outward from the particle.

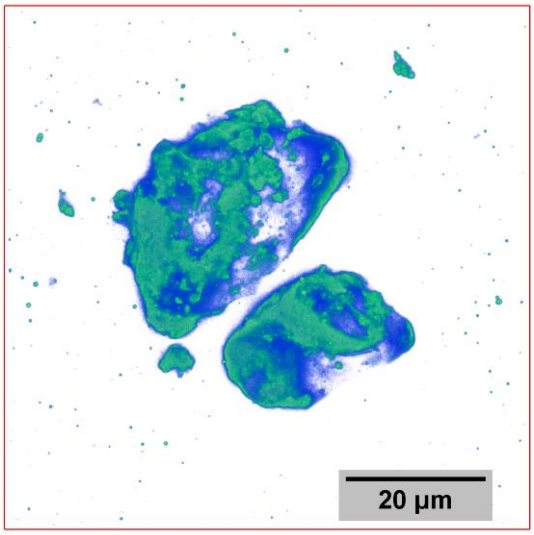

Figure 11 Cement grains in false colour representation (w/b = 0.5, 1 wt.% PCE) after hydration of 20 minutes

4 Conclusion and Outlook

The results shown here demonstrate the extension of fluorescence staining to another admixture of the plasticizer class. By fixing a substrate in a hard embedding layer, both the adsorption and desorption of stained admixtures from a liquid phase on the substrate can be studied. It can be qualitatively stated that the desorption of superplasticizer/plasticizer in a binder system is not important as it appears to be slower than the hardening of the material. This finding can be used to create permanent specimens that can be used to gain unprecedented insight into the adsorption of a plasticizer/plasticizer using CLSM.

Extending the studies on permanent preparations to other binders and activation solutions is a next step that will further elucidate the differences in the mode of action of superplasticizers between cementitious systems and AAM. By looking at well-defined pastes in the case of permanent preparations, it would also be possible to quantify the signal using a second method such as TOC. In this way, sorption isotherms can be recorded and compared. However, measurements on the specimens used are not limited to fluorescence and simple confocal laser scanning microscopy. For example, the suspected ettringite crystals could be detected by superresolution microscopy (SRM), which allows a resolution down to 10-20 nm [24, 25].

Acknowledgements

This project is funded by the Deutsche Forschungsgemeinschaft (DFG), grant number 460294323. The authors thank Prof. Plank and Dr. Lei of the Department of Chemistry at the TU Munich for providing the PCEs and Lignosulfonate.

References

[1] Sousa, V.; Bogas, J. A.; Real, S.; Meireles, I.; Carriço, A. (2023) *Recycled cement production energy consumption optimization.* Sustainable Chemistry and Pharmacy 32, p. 101010.

[2] Provis, J. L. (2018) *Alkali-activated materials.* Cement and Concrete Research 114, p. 40–48.

[3] Singh, N. B; Middendorf, B. (2020) *Geopolymers as an alternative to Portland cement: An overview.* Construction and Building Materials 237, 117455.

[4] Cunningham, P. R.; Miller, S. A. (2020) *Quantitative Assessment of Alkali-Activated Materials: Environmental Impact and Property Assessments.* J. Infrastruct. Syst. 26, p. 3.

[5] Samarakoon, M. H.; Ranjith, P. G.; Hui Duan, W.; Haque, A.; Chen, B. K. (2021) *Extensive use of waste glass in one-part alkali-activated materials: Towards sustainable construction practices.* Waste management (New York, N.Y.) 130, p. 1–11.

[6] Glanz, D.; Sameer, H.; Göbel, D.; Wetzel, A.; Middendorf, B.; Mostert, C.; Bringezu, S. (2023) *Comparative Environmental Footprint Analysis of Ultra-High Performance Concrete using Portland Cement and Alkali-Activated Materials.* Front. Built Environ. 9, p. 86.

[7] Lei, L.; Hirata, T.; Plank, J. (2022) *40 years of PCE superplasticizers - History, current state-of-the-art and an outlook.* Cement and Concrete Research 157, 106826.

[8] Kalina, L.; Bílek, V.; Hrubý, P.; Iliushchenko, V.; Kalina, M.; Smilek, J. (2022) *On the action mechanism of lignosulfonate plasticizer in alkali-activated slag-based system.* Cement and Concrete Research 157, 106822.

[9] Bakharev, T.; Sanjayan, J. G.; Cheng, Y.-B. (2000) *Effect of admixtures on properties of alkali-activated slag concrete.* Cement and Concrete Research, 1367–1374.

[10] Lei, L.; Zhang, Y. (2021) *Preparation of isoprenol ether-based polycarboxylate superplasticizers with exceptional dispersing power in alkali-activated slag: Comparison with ordinary Portland cement.* Composites Part B: Engineering 223, 109077.

[11] Li, R.; Lei, L.; Sui, T.; Plank, J. (2021) *Effectiveness of PCE superplasticizers in calcined clay blended cements.* Cement and Concrete Research 141, 106334.

[12] Andersen, P. J.; Roy, D. M.; Gaidis, J. M.; Co, W. R. G. &. (1987) *The effects of adsorption of superplasticizers on the surface of cement.* Cement and Concrete Research 17, 5, p. 805–813.

[13] Plank, J.; Winter, C. (2008) *Competitive adsorption between superplasticizer and retarder molecules on mineral binder surface.* Cement and Concrete Research 38, 5, p. 599–605.

[14] Yoshioka, K.; Tazawa, E.; Kawai, K.; Enohata, T. (2002) *Adsorption characteristics of superplasticizers on cement component minerals.* Cement and Concrete Research 32, 10, p. 1507–1513.

[15] Zhang, Y.-R.; Kong, X.-M.; Lu, Z.-B.; Lu, Z.-C.; Hou, S.-S. (2015) *Effects of the charge characteristics of polycarboxylate superplasticizers on the adsorption and the retardation in cement pastes.* Cement and Concrete Research 67, p. 184–196.

[16] Arend, J.; Wetzel, A.; Middendorf, B. (2018) *In-situ investigation of superplasticizers: From fluorescence microscopy to concrete rheology.* Cement and Concrete Research 113, p. 178–185.

[17] Adler, E. (1957) *Structural Elements of Lignin.* Industrial and Engineering Chemistry, 49, p. 1377–1383.

[18] Arend, J.; Wetzel, A.; Middendorf, B. (2020) *Fluorescence Microscopic Investigations of the Retarding Effect of Superplasticizers in Cementitious Systems of UHPC.* Materials (Basel, Switzerland) 13, p. 5.

[19] Wetzel, A.; Link, J.; Middendorf, B. (2022) *Adsorption of PCE in alkali-activated materials analysed by fluorescence microscopy.* Journal of microscopy 286, 2, p. 79–84.

[20] Brewer, L. R.; Bianco, P. R. (2008) *Laminar flow cells for single-molecule studies of DNA-protein interactions.* Nature methods 5, 6, p. 517–525.

[21] Arend, J.; Wetzel, A.; Middendorf, B. (2018) *In-situ-investigation of superplasticizer-particle-interaction by fluorescence microscopy.* Materials Today: Proceedings 5, 7, p. 15292–15297.

[22] Wetzel, A.; Glotzbach, C.; Maryamh, K.; Middendorf, B. (2015) *Microstructural investigations on the skinning of ultra-high performance concrete.* Cement and Concrete Composites 57, p. 27–33.

[23] Ferrari, L.; Bernard, L.; Deschner, F.; Kaufmann, J.; Winnefeld, F.; Plank, J. (2012) *Characterization of Polycarboxylate-Ether Based Superplasticizer on Cement Clinker Surfaces.* J. Am. Ceram. Soc. 95, 7, p. 2189–2195.

[24] Yamanaka, M.; Smith, N. I.; Fujita, K. (2014) *Introduction to super-resolution microscopy.* Microscopy (Oxf) 63, 3, p. 177–192.

[25] Schermelleh, L.; Ferrand, A.; Huser, T.; Eggeling, C.; Sauer, M.; Biehlmaier, O.; Drummen, G. P. C. (2019) *Super-resolution microscopy demystified.* Nat Cell Biol 21, 1, p. 72–84.